Biol Invasions (2021) 23:1231–1247
https://doi.org/10.1007/s10530-020-02432-0

ORIGINAL PAPER

Mapping *Phragmites* cover using WorldView 2/3 and Sentinel 2 images at Lake Erie Wetlands, Canada

Prabha Amali Rupasinghe · Patricia Chow-Fraser

Received: 23 May 2020 / Accepted: 4 December 2020 / Published online: 3 January 2021

Abstract *Phragmites australis* (Cav.) Trin. ex Steudel subspecies *australis* is an aggressive plant invader in North American wetlands. Remote sensing provides cost-effective methods to track its spread given its widespread distribution. We classified *Phragmites* in three Lake Erie wetlands (two in Long Point Wetland Complex (LP) and one in Rondeau Bay Marsh (RBM)), using commercial, high-resolution (WorldView2/3: WV2 for RBM, WV3 for LP) and free, moderate-resolution (Sentinel 2; S2) satellite images. For image classification, we used mixture-tuned match filtering (MTMF) and then either maximum likelihood (ML) or support vector machines (SVM) classification methods. Using WV2/3 images with ML classification, we obtained higher overall accuracy for both LP sites (93.1%) compared with the RBM site (86.4%); both *Phragmites* users' and producers' accuracies were also higher for LP (89.3% and 92.7%, respectively) compared with RBM (84.3% and 88.4%, respectively). S2 images with SVM classification provided similar overall accuracies for LP (74.7%) and for the RBM (74.3%); *Phragmites* users' and producers' accuracies for LP were 85.3% and 76.3%, and for the RBM, 69.1% and 79.2%, respectively. Using WV2/3, we could quantify small patches (percentage cover $\geq$ 20%; shoots $\geq$ 1 m tall; stem counts $>$ 25) with accuracy $>$ 80%, whereas parallel effort with S2 images only accurately quantified high density ($>$ 60% cover), mature shoots ($>$ 1 m tall; Stem counts $>$ 100). By simultaneously mapping young or sparsely distributed *Phragmites* shoots and dense mature stands accurately, we show our approach can be used for routine mapping and regular updating purposes, especially for post-treatment effectiveness monitoring.

Keywords MTMF · *Phragmites* · WorldView 2 and WorldView 3 · Sentinel 2 · Wetlands · Invasive species

Introduction

Phragmites australis (the common reed; hereafter *Phragmites)* is a taxonomically diverse perennial grass, with 27 genetically distinct groups throughout the world, 11 of which are found in North America. One of the European haplotypes, M, is an aggressive invader in coastal wetlands and roadway corridors and have been growing at the expense of native vegetation in many coastal marshes of the lower Great Lakes (Saltonstall 2002). This haplotype exhibits invasive characteristics, including its ability to aggressively colonize exposed mud flats sexually (through seeds), and then expand asexually (through rhizomes) to form

P. A. Rupasinghe (✉) · P. Chow-Fraser
Department of Biology, McMaster University, 1280 Main St. West, Hamilton, ON L8S 4K1, Canada
e-mail: rupasinp@mcmaster.ca

dense monocultures that inhibit biodiversity of other plants and wildlife (Meyerson et al. 2000; Markle and Chow-Fraser 2018). Its rapid spread has been attributed to it being a superior competitor against other emergent vegetation (Meyerson et al. 2000; Uddin et al. 2014) and to being more tolerant of disturbances (e.g. road maintenance and changes in hydrologic regimes) and environmental stressors (e.g. increased salinity due to road de-icing salts) (McNabb and Batterson 1991; Marks et al. 1994; Chambers et al. 1999; Brisson et al. 2010; Taddeo and Blois 2012; Rodríguez and Brisson 2015). Once established, this aggressive invader has been known to reduce wetland plant diversity and alter vegetation structure (Ailstock et al. 2001; Mal and Narine 2004; Lambert et al. 2010; Gilbert et al. 2014), habitat for wetland fauna (Weinstein and Balletto 1999; Bolton and Brooks 2010; Gilbert et al. 2014; Cook et al. 2018; Markle and Chow-Fraser 2018), and modify hydrology and soil properties (Chambers et al. 1999; Bolton and Brooks 2010), thus having an overall negative impact on ecosystem functions.

Optimal conditions for the growth of *Phragmites* are provided by water bodies with seasonal fluctuations of 30 cm (Deegan et al. 2007). New shoots of *Phragmites* arise in the spring and may grow up to 3–4 m tall during the summer, producing large inflorescences giving rise to thousands of seeds towards the late summer and early fall (Burgess and Evans 1989; Gilbert et al. 2014; Gagnon Lupien et al. 2015). According to Albert et al. (2015), both seeds and vegetative propagation contribute to the new *Phragmites* establishment; however, 84% of the newly established *Phragmites* stands are formed through seed germination. Lathrop et al. (2003) have reported three patterns of *Phragmites* growth in brackish tidal marshes at eastern USA: (a) colonization or new growth, (b) linear clonal growth along an axis, and (c) circular clonal patches (non-directional) with random spread. New *Phragmites* stands are characterized by low-density short shoots with a few small leaves. *Phragmites* grown in deep water also produce lower number of shoots and shorter rhizomes, thus limiting its vegetative expansion (Weisner and Strand 1996; Vretare et al. 2001). Linear *Phragmites* stands are mostly observed along the roadside in linear wetland corridors and along shores of water ways, while circular growths are mostly observed in wetlands with ideal growth conditions.

The distinctive growth patterns of *Phragmites* make them well suited to remote sensing approaches. A number of methods have been developed to map dense *Phragmites* with higher accuracy (i.e. $> 80\%$), involving satellite images of moderate 30-m Landsat and 10-m and 20-m Sentinel 2 (Rupasinghe and Chow-Fraser 2019), and emergent vegetation with 10-m and 20-m SPOT; 4-m IKONOS (Rutchey and Vilchek 1999; Sawaya et al. 2003; Phillips et al. 2005). Other methods are available that employ more expensive high resolution hyperspectral images acquired by commercial sensors such as AVIRIS, CASI, HyMap, and PROBE-1 (Schmidt and Skidmore 2001; Bachmann et al. 2002; Williams and Hunt 2002; Lopez et al. 2004), that could be used for mapping low-density stands. For mapping invasive species, multispectral images have advantages over hyperspectral images because of their overall lower cost (some available at no cost or reduced cost), higher spatial coverage, and shorter durations between acquisitions that facilitate repeated mapping of the entire wetland for assessing treatment efficacy at the ecosystem scale. The main disadvantage, however, is that multispectral images produce lower accuracy compared with hyperspectral images, especially at early stages of invasion when plant densities are low (Adam et al. 2010).

Selection of hyperspectral or multispectral images and choosing the best classification algorithm is essential for accurate species-level mapping. Campbell (2002) described two categories of classification algorithms that can be used in supervised classification methods: (a) distance based or hard classifiers and (b) unmixing based or soft classifiers. In hard classifiers, the distance from a known reflectance value is used to determine the match between an unknown pixel. Maximum likelihood classification (ML), spectral angle mapper (SAM), and minimum distance classification are some of the examples for hard classifiers and they act as 'first look' tools to identify the presence of target species in the study area (Campbell 2002). The soft classifiers such as linear spectral unmixing (LSU), mixture tuned match filtering (MTMF), and Bayesian probability use relative abundance of land cover classes within a pixel. In these techniques, mixed pixels that contain several landcover classes are decomposed into its original constituents, to develop a set of output images rather

than a single classified image as in hard classifiers (Lass et al. 2005; Williams and Hunt 2004, 2002).

Despite the expansion of *Phragmites* in many Lake Ontario and Erie coastal marshes in the late 1990s (Wilcox et al. 2003), control programs were not implemented in Ontario until 2007 (Bourgeau-Chavez et al. 2015; Gilbert 2015). Non-chemical control methods such as cutting, drowning, smothering, covering, excavating, plowing, grazing, and burning have been tested in Ontario with varying success (Gilbert et al. 2014). In some instances, mechanical control cannot be implemented in natural ecosystems when the invaded area is large and inaccessible by either boat or road. In these instances, aerial application of either glyphosate or imazapyr has been used (Avers et al. 2007; Derr 2008; Gilbert et al. 2014; Gilbert 2015). Although glyphosate had been used widely within the United States to control the growth of invasive *Phragmites* (Gilbert 2015), its use in Ontario has been prohibited except by Emergency Use Registration, which requires first, an accurate map of *Phragmites* in the wetland to spray only the target area during aerial herbicide application and to avoid spraying on native vegetation and secondly, an accurate monitoring program to quantify the efficacy of the treatment program since complete removal of *Phragmites* in an area requires repeated applications over several years (Gilbert et al. 2014; Rupasinghe et al. 2017).

To meet treatment protocols such as Ontario's Emergency Use Registration requirements, managers must obtain high mapping accuracies for both the expansive mature stands of *Phragmites* (i.e. untreated) as well as the small, young, sparsely distributed shoots (i.e. when they regenerate following treatment). Such mapping would require a remote-sensing approach that is cost-effective, repeatable, and produce results that maximize both producers' (mapping accuracy on the map makers' or the producers' perspective, complements the level of omission error or the false negatives) and users' (mapping accuracy on the map users' perspective, complements the level of commission error or the false positives) accuracies, since both false negatives and false positives are unacceptable at high levels. In this study, we compare classification accuracies associated with two multispectral products (commercially available, high resolution WorldView 2/WorldView3 (WV 2/3) and the freely available, moderate resolution Sentinel 2 (S2) images) using sub-pixel image classification methods to determine the relative usefulness of these image products for mapping the distribution of *Phragmites* in three Lake Erie marshes that had been colonized since the late 1990s (Wilcox et al. 2003). At the time of image acquisition, the patterns of *Phragmites* distribution varied across the three sites. One wetland had low-density stands of young shoots a year following herbicide treatment, whereas another had large, dense mature *Phragmites* stands that had not yet been chemically treated, and a third had a mixture of both chemically treated and untreated areas. Our goal is to experiment with sub-pixel techniques used previously, mostly with hyperspectral images, and apply them to multispectral images to obtain accuracies $> 80\%$ for all *Phragmites* density classes across the three Lake Erie wetlands.

Methods

Study sites

Two of the three Lake Erie wetlands, Big Creek National Wildlife Area (BCNWA; 42° 35′ N 80° 27′ W) and Crown Marsh (CM; 42° 35′ N 80° 24′ W) occur in Long Point (LP) Wetland Complex, which is internationally recognized as an UNESCO World Biosphere Reserve and under the Ramsar Convention as an internationally important wetland (Ministry of Natural Resources and Forestry 2019) (Fig. 1). BCNWA covers an area of 771 ha and consist of the Big Creek unit (615 ha) and the Hahn Marsh Unit (156 ha). It is federally owned and managed by the Environment and Climate Change Canada. CM is about 2 km East to the BCNWA and covers approximately 708.2 ha. It is owned by the Province of Ontario and is normally accessible to the public throughout the year. These wetlands are characterised by emergent aquatic vegetation, mainly Cattail (*Typha* sp.), *Phragmites*, and Bulrushes (*Juncus* sp.) (Long Point Crown Marsh Rehabilitation Steering Committee 2007) and meadow marsh dominated by *Calamagrostis canadensis* (Yuckin and Rooney 2019). The third wetland, Rondeau Bay Marsh (RBM; 42° 17′ N 81° 52′ W), is managed by the province of Ontario, and is located further west on the north shore of Lake Erie, covering an area of 1800 ha (Fig. 1). RBM is characterized by Carolinian forests, sandy peninsula, and marsh (Mann and Nelson 1980). The drier parts of

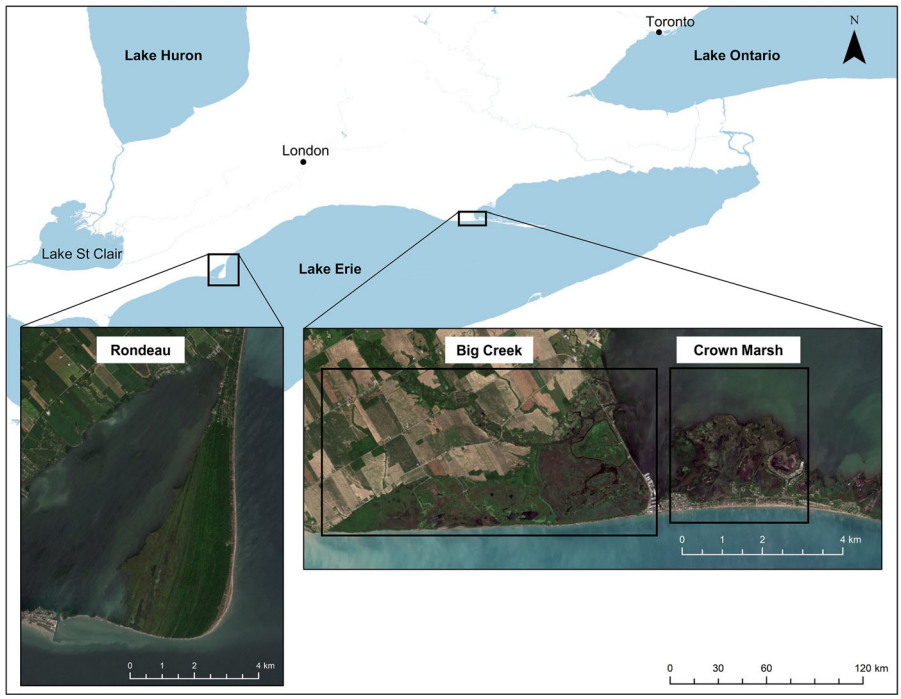

Fig. 1 Map of the study sites located in the north shore of Lake Erie

the marsh are dominated by *Cephalanthus occidentalis*, *Salix*, and *Cornus* spp. Other than *Phragmites*, the emergent plants included monocultures of *Typha latifolia*, *T. angustifolia*, *T.* x *glauca* and *Zizania aquatica* and the marshes with deeper standing water was dominated by aquatic species of Cyperaceae, *Nuphar advena,* and *Nymphaea odorata* (Finkelstein and Davis 2006).

Remote sensing data

WV, which is operated by DigitalGlobe, is a fourth-generation, optical and commercial earth-observation satellite series, with the highest spatial resolution (30 cm for WV3 and 40 cm for WV2) of all existing optical satellites available for research (Kurihara et al. 2018). WV3 has revisit frequency less than 1 day at 40°N latitude and 4.5 days at 20° off-nadir or less while for WV2, revisit frequency is 1.1 days and 3.7 days at 20° off-nadir (Satellite Image Corporation 2017). A cloud-free WV3 image was acquired on 4th July 2018 for BCNWA and CM sites and WV2 image was acquired on 5th September 2018 for RBM site. WV3 images consist of one panchromatic band (445–808 nm spectral resolution and 30 cm spatial resolution) and eight multispectral bands (1.2 m spatial resolution), including the coastal blue (397–454 m), blue (445–517 nm), green (507–586 nm), yellow (580–629 nm), red (626–696 nm), red edge (698–749 nm), Near Infra-Red 1 (NIR 1; 765–899 nm) and NIR 2 (857–1039 nm) bands. For the WV2 images, the panchromatic band is 40 cm spatial resolution (464–801 nm) with 8 multispectral bands (1.8 m spatial resolution); coastal blue (401–453 m), blue (447–508 nm), green (511–581 nm), yellow (588–629 nm), red (629–689 nm), red edge (704–744 nm), NIR 1 (772–890 nm) and NIR 2 (862–954 nm) (Nikolakopoulos and Oikonomidis 2015).

S2 is a satellite owned by the European Space Agency (ESA), designed for studies based on terrestrial observations. It consists of two satellites, Sentinel-2A (launched in 2015) and Sentinel-2B (launched in 2017). S2 provide revisit time of 5 days at the equator (European Space Agency 2020). The images for BCNWA and CM sites were acquired on 6th July 2018 and for RBM site on 28th August 2018. S2 images consist of four 10-m resolution bands (Blue; 490 nm, Green; 560 nm, Red; 665 nm, and

NIR; 842 nm), six 20-m resolution bands (Vegetation red edge; 705 nm, 74 nm, 783 nm, Narrow NIR; 865 nm, Short Wave InfraRed 1 (SWIR 1); 1610 nm, SWIR 2; 2190 nm), and three 60-m resolution bands (Coastal aerosols; 443 nm, Water vapor; 945 nm, and SWIR Cirrus; 1375 nm).

Ground truth data

We conducted field sampling in the summers of 2018 and 2019 at the BCNWA and CM to record locations of *Phragmites* as ground truth data. In the field, we established 1.5 × 1.5 m quadrats in the *Phragmites* patches and visually recorded percentage cover of *Phragmites*. Then we cut all the standing *Phragmites* stems within the quadrat and weighed them using a Xcalibur Spring Scale. Stand height of *Phragmites* was estimated by cutting down the tallest shoot at its base, laying it on the ground, and measuring them with a tape measure (to the nearest cm). We recorded the coordinates of the quadrats using Garmin eTrex handheld GPS (Garmin and subsidiaries). In total for both years, we collected *Phragmites* information from 58 quadrats in BCNWA and 89 quadrats in CM. In addition to field sampling, we used high-resolution image interpretation to identify land-cover classes on inaccessible areas. We used the sensefly eBee (Parrot, Cheseaux-Lausanne, Switzerland (SenseFly 2020a), equipped with the Parrot Sequoia + camera (SenseFly 2020b) to acquire Unmanned Aerial Vehicle (UAV; 13 cm resolution) images in July 2019. We used this high-resolution UAV image and the pan-sharpened WV3 image (30 cm spatial resolution; same image used in image classification) to collect ground reference for land-cover classes for both classification and accuracy assessment for areas with limited access. We identified these classes through both knowledge in the field and visual comparison of manually digitized UAV image acquired in late summer 2015 (Marcaccio et al. 2016). In addition, we also used 15 *Phragmites* treatment locations corresponding to a spraying program conducted between September and October in 2018 by Nature Conservancy Canada (NCC) to validate the image classification.

Field data used as ground reference for RBM were collected by Angoh et al., (841 quadrats; unpublished data) as part of their study to examine the effect of *Phragmites* on turtle habitats. They used 2 × 2 m quadrats and counted the number of dead and live *Phragmites* stems and Cattail stems within the quadrat and recorded the dominant species and landcover types within the quadrat. Of these 841 quadrats, 313 contained *Phragmites*. In addition to the field data, we used locations from manual interpretation of pan-sharpened WV2 image (40 cm spatial resolution, same image used for the image classification) and obtained 10 locations where *Phragmites* had been treated in 2018 (data provided by Ontario Parks).

Remote sensing data processing

We conducted all image pre-processing and processing with the software ENVI 5.5 (L3Harris Geospatial 2020). We performed radiometric correction and atmospheric correction (ENVI FLAASH correction) to obtain surface reflectance values for both WV2/3 and S2 images. Reflectance values were rescaled from 0 to 1 after FLAASH correction. For S2 images, we separately preprocessed the 20-m resolution bands, resampled them to 10-m resolution and stacked them with the preprocessed 10-m bands prior to image analysis.

We performed sub-pixel image classification using spectral mixture analysis to detect *Phragmites*. In the spectral mixture analysis, it is assumed that the mixed pixel spectrum is a linear combination of the spectral signatures of the component classes of the pixel (Adams et al. 1985). Mixture tuned match filtering (MTMF) is a method used in spectral mixture analysis which performs partial spectral unmixing (Boardman et al. 1995). In this technique, only the pure spectral signature (endmember) of the target landcover class needs to be defined. The image is then filtered for the defined endmember spectrum and the unknown background spectra are supressed (Boardman 1998; Boardman and Kruse 2011; Brelsford and Shepherd 2013). The three steps in MTMF includes: (a) minimum noise fraction (MNF) transformation to minimize and decorrelate noise, (b) match filtering (MF) to estimate the abundance of the target class, and (c) mixture tuning (MT) to separate false positives from the MF step (Boardman 1998; Boardman and Kruse 2011). The MTMF produces two outputs at the end of the analysis, the MF score image, and the infeasibility image. The MF score represents the relative abundance of the target class within a pixel. It ranges from 0 to 1 where a score of 1 represents a perfect match

between the end member and the sub-pixel abundance or 100% of the target class within the pixel. The infeasibility scores are in noise sigma units and provide the feasibility of the MF results (Harris Geospatial Solutions, Inc 2020).

First, we performed minimum noise fraction (MNF) transformation for both pre-processed WV2/3 and S2 images to reduce image dimensionality. After the MNF transformation, we performed the MTMF followed by image classification. We evaluated the eigen value plots and the classification results with various combinations of MNF bands and based on these results, chose the first four or five bands for further analysis (additional MNF bands added unwanted noise to the classification). For the MTMF, we extracted spectral endmembers using the field observations. Again, we repeated the classification with *Phragmites* endmember alone and with different combinations of endmembers of the other classes and checked for accuracy. Then we selected the endmember combination that provided the highest classification accuracy.

After the MTMF transformation, we classified the images using both maximum likelihood (ML) and support vector machines (SVM) classification methods. We applied 5 × 5 majority filter for all classes except for *Phragmites* and then compared the results. For image classification and endmember extraction, we used *Phragmites* locations collected in the field in addition to locations obtained from the image interpretation (73 locations for the LP and 38 locations for the RBM); we used all *Phragmites* quadrat data collected in the field and the *Phragmites* treatment locations for accuracy assessment (162 locations for the LP and 323 locations for the RBM). Therefore, there was no overlap between classification and accuracy assessment locations.

After image classification, we imported landcover maps that provided the highest mapping accuracy into ArcMap 10.4.1 and evaluated the mapping accuracy of *Phragmites* cover, stem count, height, and weight using the quadrat data collected during field work. To enable analyses, we divided percentage cover data into five equal intervals (i.e. 20% increments). Height information were sorted into four categories (< 1 m, 1–2 m, 2–3 m, and > 3 m) as were weight data (0–2 kg, 2–4 kg, 4–6 kg, and > 6 kg). Although we performed image classification of BCNWA and CM together (i.e. a single image was acquired for both sites), we calculated percent cover and analyzed the height and weight data separately for the two sites. For the RBM site, we sorted the live stem counts per quadrat into six categories (0, 1–25, 25–50, 50–75, 75–100, and > 100), before calculating mapping accuracies.

We used Fragstats 4.2 to extract patch area, largest patch index (LPI), and radius of gyration of each patch for the three sites separately using the maps with highest classification accuracy. We analysed the data using the JMP 15 software and created plots in MS Excel and in JMP.

Results

Phragmites and wetland land cover mapping

After analyzing different endmember combinations, we obtained the highest classification accuracy with the combination that included *Phragmites*, trees/shrubs (mixed forest for RBM site), and open land. Accuracy obtained for this combination was higher than that for the *Phragmites* endmember alone. Therefore, we used this combination of classes for the rest of the study (i.e. all combinations of sites and sensors).

For the BCNWA and CM sites, we classified the image into eight land cover classes; *Phragmites*, Cattail organic shallow marsh, mixed organic shallow marsh, trees/shrubs, open land, open water, submerged shallow aquatic shallow marsh, and floating vegetation (Fig. 2). We classified the RBM site also into eight classes: *Phragmites*, Cattail organic shallow marsh, floating vegetation, meadow marsh, mixed forest, open land, open water, and organic thicket swamp (Fig. 3). The overall, user's and producer's accuracies were higher for WV2/3 than for S2, regardless of classification method (Table 1). For WV2/3 images only, ML classification produced higher classification accuracy than did SVM. The SVM classification resulted in high commission error of *Phragmites* for both LP and RBM sites (Table 1; Figs. 2, 3). By comparison, SVM produced higher accuracy than did ML classification for S2 images. Based on these results, we used the ML classification for the WV2/3 images and SVM classification for the S2 images in *Phragmites* cover, stem count, height, and weight analysis.

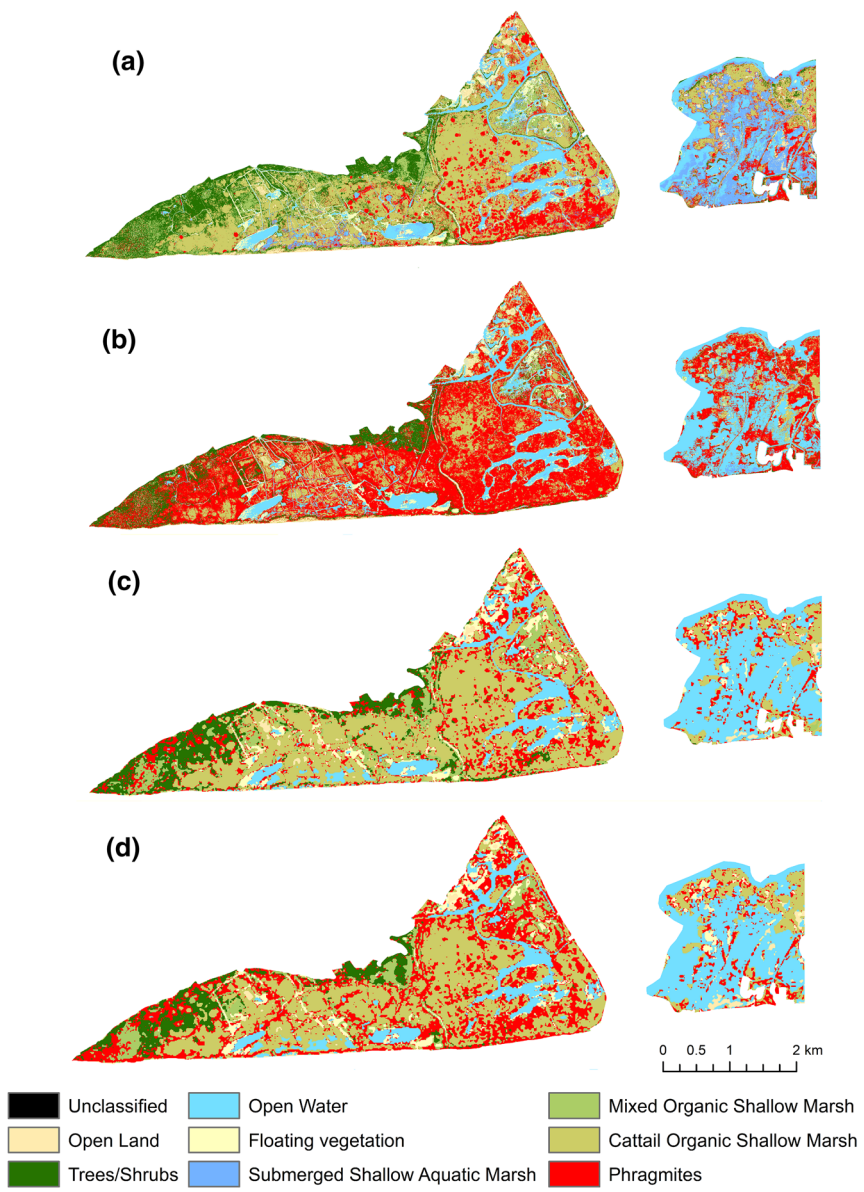

Fig. 2 Classified images of BCNWA and CM sites with **a** WV3 images-ML classification, **b** WV3 images-SVM classification, **c** S2 images-ML classification and **d** S2 images-SVM classification

Phragmites percentage cover and stem count analysis

The MF score of *Phragmites* increased with percentage cover and stem count (Figs. 4, 5); however, whereas significant positive regressions between MF score and percentage cover were found for all WV2/3 images, only the S2 image for BC was associated with a significant regression. Classification of S2 images were generally associated with comparatively low accuracies (Table 1), with no significant positive correlation between MF scores and percentage cover or stem counts (Figs. 4, 5). Despite the statistical significance, the regression coefficient between the MF score and percentage cover of *Phragmites* was relatively low (Fig. 4). This is due to the spectral similarities between *Phragmites* and other vegetation classes. We observed lower MF scores for some

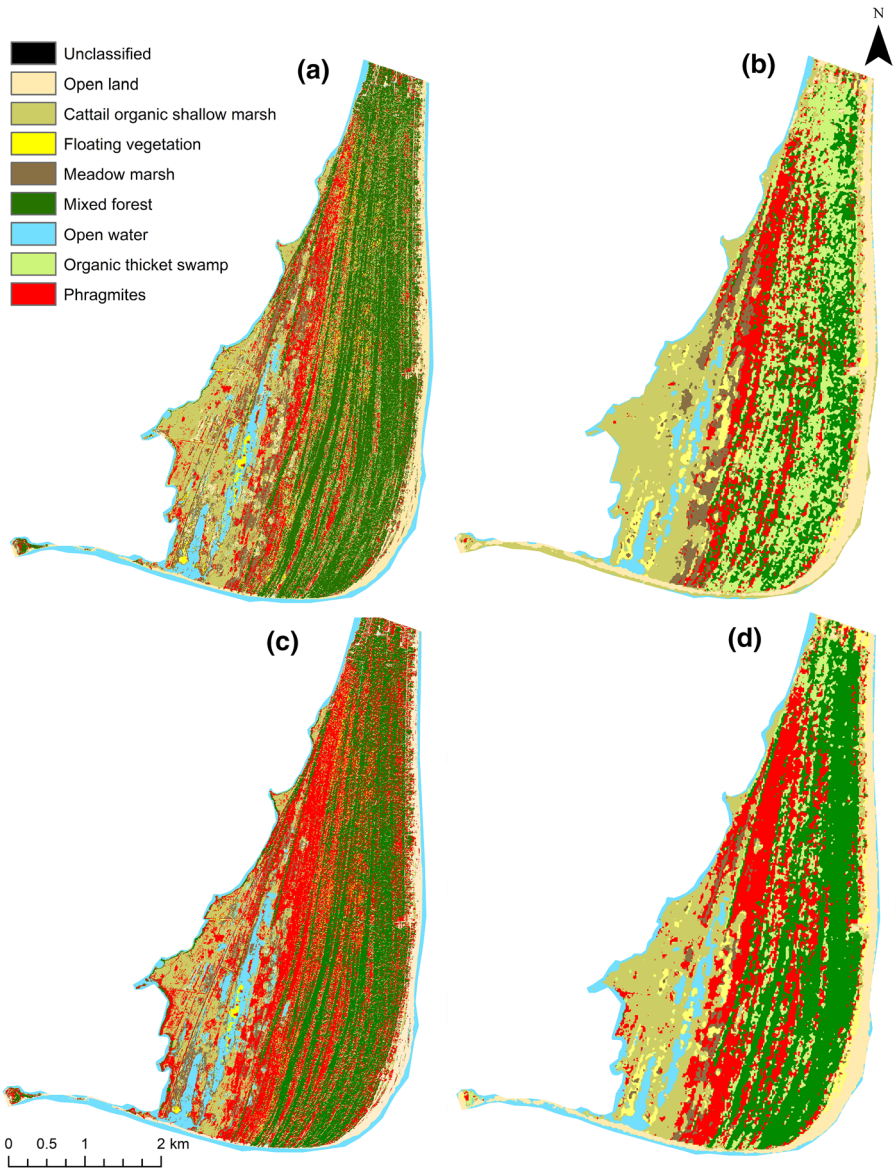

Fig. 3 Classified images of RBM site with **a** WV2 images-ML classification, **b** S2 images-ML classification, **c** WV2 images-SVM classification and **d** S2 images-SVM classification

locations with 100% *Phragmites* cover (as reported in the field) because the actual image pixels could be mixed with different reflectance signals such as shadows cast by *Phragmites* itself or by adjacent taller vegetation, non-leaf reflectance from large inflorescences, dried leaves and stalks, glare from open water etc. We observed a similar trend with the stem count data for the RBM site, in which the regression coefficient between MF score and the live stem count of *Phragmites* was very low (Fig. 5). The dead stems in majority of the quadrats at the RBM site and other reflectance signals associated with non-*Phragmites* vegetation may explain the low range of MF scores.

Although accuracies for the five density categories varied for the two LP sites, some generalizations can be made. First, regardless of the site, we obtained higher accuracies with the WV3 image (Fig. 6a, b) than with the S2 image (Fig. 6c, d). Secondly, in all cases, the lowest density category (< 20% cover)

Table 1 Overall, *Phragmites* users' and producers' accuracy for different combinations of WV2/3 and S2 images and SVM and ML classification methods

Site	Classification accuracy	WV3		S2	
		SVM	ML	SVM	ML
BCNWA and CM	Overall accuracy %	69.75	**93.08**	**74.68**	72.15
	Kappa	0.6162	**0.9062**	**0.6832**	0.6467
	Phragmites Producers' accuracy %	95.07	**92.72**	**76.32**	79.82
	Phragmites Users' accuracy %	41.77	**89.29**	**85.29**	79.13
Site	Classification accuracy	WV2		S2	
		SVM	ML	SVM	ML
RBM	Overall accuracy %	75.77	**86.37**	**74.25**	70.86
	Kappa	0.6869	**0.8220**	**0.6927**	0.6503
	Phragmites Producers' accuracy %	95.14	**88.43**	**79.17**	48.57
	Phragmites Users' accuracy %	61.94	**84.29**	**69.09**	70.15

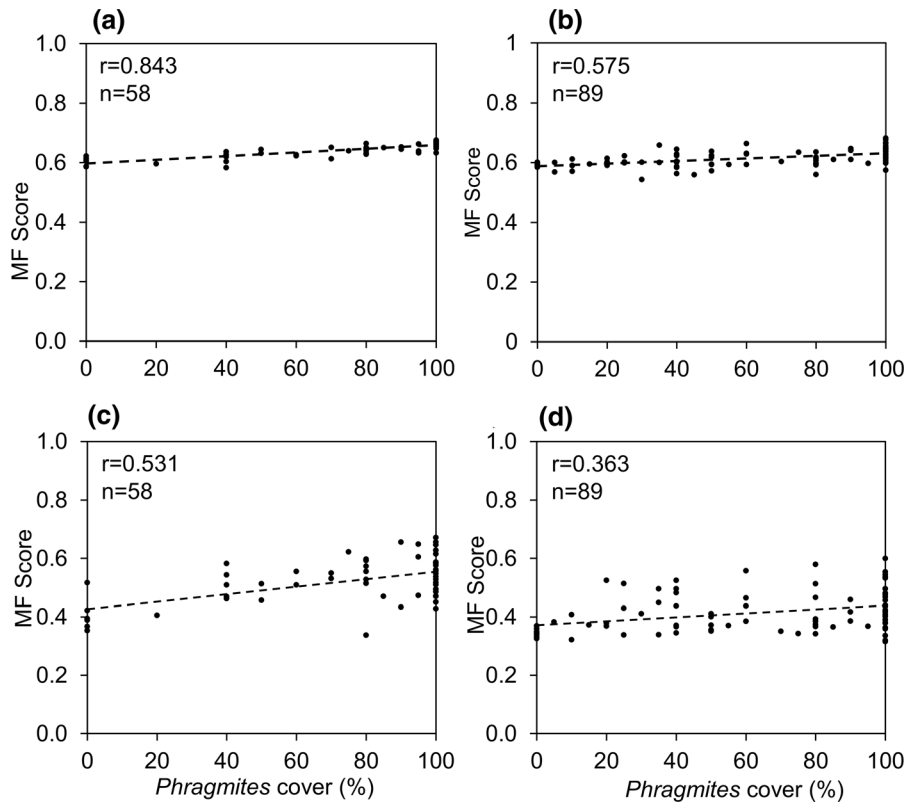

Fig. 4 Linear regression plots of MF scores versus *Phragmites* percent cover associated with WV3 images for **a** BCNWA and **b** CM sites; corresponding regression plots associated with S2 images for **c** BCNWA and **d** CM sites

failed to meet the threshold accuracy of 80% (Fig. 6). For BCNWA, four of the remaining density categories achieved acceptable accuracies with the WV3 image compared with three with the S2 image (Fig. 6a vs. c). Inaccurate classifications for the highest density (80–100% cover) were caused by confusion between *Phragmites* and Cattail and in a few cases, between a patch of high-density *Phragmites* and trees/shrubs. For CM, acceptable accuracies were only achieved with the WV3 image in the two highest density categories, whereas all accuracies were $< 80\%$ with the S2 image (Fig. 6b vs. d).

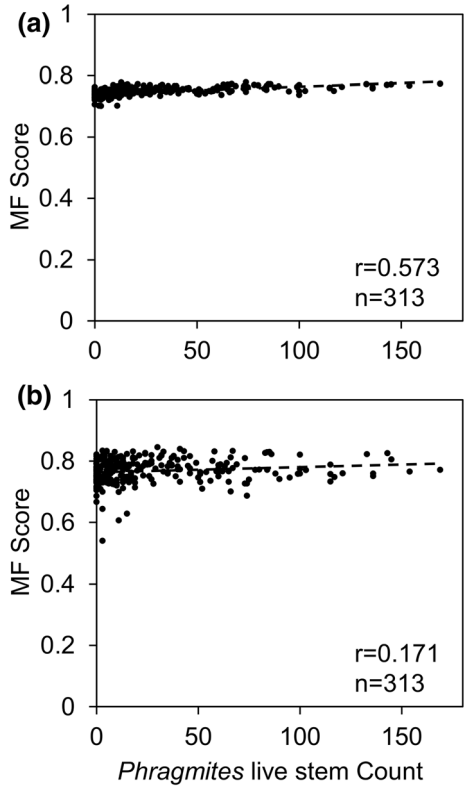

Fig. 5 Linear regression plots of MF scores versus *Phragmites* stem counts obtained with **a** WV2 and **b** S2 images for the RBM site

For the RBM site, we had stem counts instead of percentage cover data. The WV2 image yielded > 80% accuracies for quadrats with greater than 25 *Phragmites* stems (Fig. 7). An accuracy of 93.3% was obtained for quadrats with over 100 live *Phragmites* stems, and 53.4% for the lowest category with fewer than 25 live stems. For quadrats containing non-living *Phragmites* stems, we obtained an accuracy of 50.0%. For S2 images, accuracy for the highest count category (> 100 live stem) was only 73.3% (4 of 15 quadrats had been misclassified), and accuracies for all other categories were lower than 65%.

We observed a significant positive correlation between percentage cover of *Phragmites* and live stem weight and height for both BCNWA ($r = 0.58$ and $r = 0.71$ respectively) and CM ($r = 0.84$ and $r = 0.79$ respectively) sites. Therefore, we analysed the classification accuracy of *Phragmites* sorted by weight and height. With the WV3 images, we found > 80% accuracy for all height categories over 1 m. We obtained accuracy of 75.0% for plants < 1 m tall at the BCNWA site (Fig. 8a). By contrast, the highest accuracy (86.7%) for the S2 image was obtained for the 1–2 m category, while plants shorter than 1 m, taller than 3 m, and between 2–3 m were associated with much lower accuracies of 62.5%, 71.4% and 82.1%, respectively (Fig. 8b). We did not have any quadrat data over 3 m height category for the CM site. We obtained 100% accuracy for the height category of 2–3 m and very low accuracy for 0–1 m height category (7.7%; Fig. 8e). We obtained a similar trend with the S2 images, where highest accuracy was obtained for the intermediate category (2–3 m; 85.7%), and lowest accuracy was obtained for quadrats with plant heights < 1 m (7.7%; Fig. 8f). Based on the results, accuracy for both WV3 and S2 images generally improved with increasing plant height.

We also compared accuracies between WV3 and S2 for classifying *Phragmites* weights in the two LP sites. For BCNWA, accuracies for all four weight categories met the target of 80% when WV3 image was used (Fig. 8c), whereas only two categories met this target when the S2 image was used (Fig. 8d). For CM, accuracies for only three of the weight categories were > 80% when WV3 image was used (Fig. 8g), whereas none of the categories had acceptable accuracies when the S2 image was used (Fig. 8h). Therefore, in general, accuracies were much better for the WV3 than the S2 image.

Phragmites patch characteristics

We studied the patch characteristics using the maps produced using the WV2/3 images as it provided the highest mapping accuracy. The patch sizes of *Phragmites* in this study ranged from very small (2 m^2) to extremely large (40 ha) patches. The two largest patches were found in RBM (40.33 ha) and in BCNWA (26.89 ha). By far, however, the majority (> 80% of the 58,081 patches) of these *Phragmites* patches were < 100 m^2 at the BCNWA site. In comparison, 70% of 17,889 *Phragmites* stands in CM and 50% of the 50,191 stands in RBM had an area < 100 m^2. The radius of gyration, which is a measure of the spatial extent of a habitat patch (defined as a mean distance between each cell in the patch and the patch's centroid) differed significantly among the three sites. RBM, with the greatest total area occupied by *Phragmites*, also had the highest

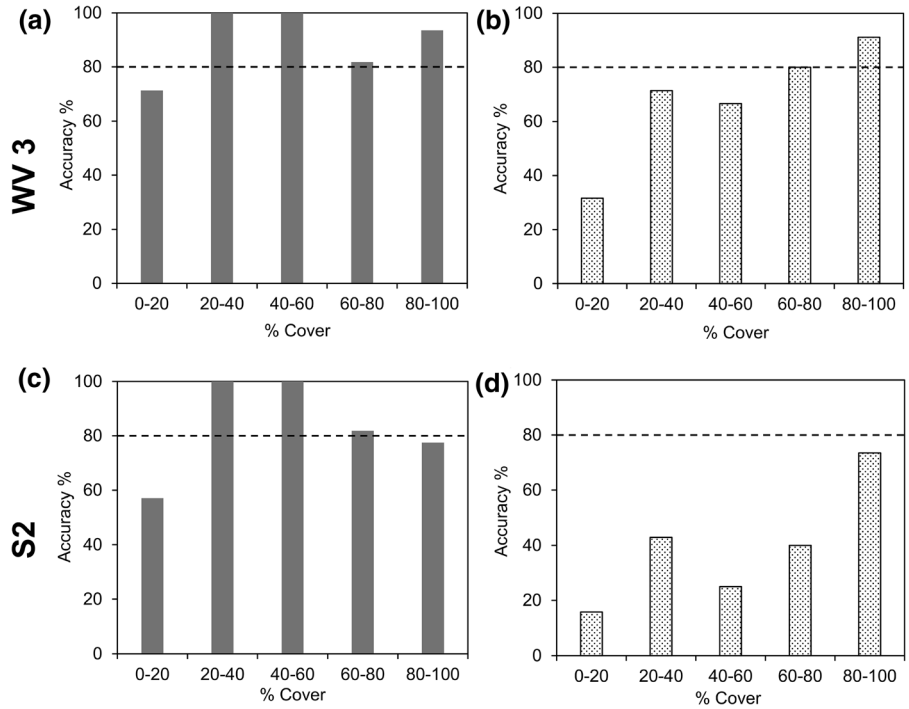

Fig. 6 Comparison of mapping accuracies for *Phragmites* in five density categories for BCNWA (solid bars) and CM (stippled bars) using ML classification with WV3 (top panels) and SVM classification with S2 images (bottom panels)

radius of gyration (Fig. 9a, b). The calculated geometric mean patch size of *Phragmites* in both LP wetlands was < 5 m^2 while that in RBM was more than double (> 10 m^2; Fig. 9c). When we compared the LPI for the three sites, CM, BCNWA, and RBM sites have 0.8%, 2.2%, and 2.5% respectively. Overall, these results indicate that the RBM site had comparatively larger *Phragmites* patches, and fewer small-sized stands compared with the LP sites.

Discussion

Our study is the first to use subpixel image classification using MTMF with multispectral satellite images to map *Phragmites*, and we have been able to achieve up to 90% accuracy across landscapes containing patches that range from very large size of 40 ha to very small sparse stands of 2 m^2. We achieved higher classification accuracy by using spectral endmembers that were defined for trees/shrubs and open land in addition to *Phragmites* instead of *Phragmites* endmember alone. We focused on developing simple, cost-effective methods that could be used in sites with a range of patch sizes and distributions so that the protocol can be repeated across many different wetlands by environmental agencies. Our goal was to obtain accurate maps of both low density or young *Phragmites* stands as well as expansive, large stands so that the same protocol can be used for initial assessment as well as effectiveness monitoring. We found that the best combination at no-cost involves the use of S2 images and SVM classification while the best combination with highest mapping accuracy involves the commercially available WV2/3 images and use of ML classification.

In all respects, classification of WV2/3 images produced higher overall and *Phragmites* accuracies than did classification of S2 images. This difference in performance is directly related to the higher spatial resolution of WV2/3 (1.8 m and 1.2 m) compared with S2 (10 m and 20 m) which results in higher spectral mixing in the latter. When we compared the two sites, RBM had slightly lower accuracy than did LP sites, and this difference also may have been due to slightly lower spatial resolution of WV2 compared with WV3. Spectral resolution may also have affected the results since we used 8 bands of WV2/3 (from 400 to 1040 nm wavelength) compared with 10 bands of

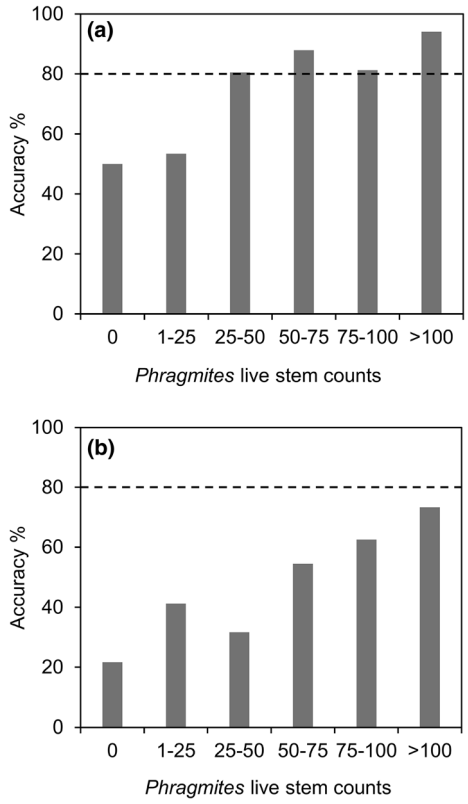

Fig. 7 Mapping accuracies of live *Phragmites* in six stem count categories for the RBM site using **a** WV2 image-ML classification and **b** S2 image-SVM classification

S2 (from 490 to 2190 nm wavelength). Although S2 images have a greater number of bands covering a larger wavelength region, the spatial resolution appeared to have considerably reduced the accuracy of image classification.

We observed some classification confusion of *Phragmites* with Cattail, open water, and trees/shrubs. In our study sites, Cattail is most similar to *Phragmites* in terms of being tall, unbranched, and forming dense monospecific stands, with somewhat similar leaf arrangement when compared to other vegetation classes. Given that they have similar habitat requirements, they are often found in mixed stands, and these morphological similarities may have resulted in similar reflectance signals that resulted in classification confusions between *Phragmites* and Cattail (Rupasinghe and Chow-Fraser 2019). Initially, we included meadow marsh in our classification for the LP sites as this is an important wetland category, but this increased *Phragmites* omission error. Meadow marsh at LP sites consisted of mixed plant species such as grasses, sedges, emergent shrubs, and upland plant species and can be highly confused with *Phragmites* when mapped with satellite images (Rupasinghe and Chow-Fraser 2019). The meadow marsh class was mostly confused with young and lower density *Phragmites* patches due to spectral similarities. Therefore, we excluded meadow marsh from the final classification of the LP sites because our main target was to improve *Phragmites* producers' and users' accuracies. Due to this modification, vegetation in the meadow marsh habitat was incorrectly classified as Cattail or mixed organic shallow marsh, but only infrequently as young, low density *Phragmites*. As our intention was to map low density *Phragmites* as accurately as possible for management purposes, missing meadow marsh was not considered a significant problem. This confusion, however, was not observed at the RBM site mainly because the *Phragmites* stands at RBM are large and dense and therefore not easily confused with spectral characteristics of meadow marsh.

We also observed misclassifications between *Phragmites* and trees/shrubs in some locations. This occurred in some extremely dense *Phragmites* patches. Confusion of *Phragmites* with open water occurred in areas where *Phragmites* was beginning to colonize in shallow water and had low plant density. Spectral reflectance of sunlight by water can also interfere with the signal produced by *Phragmites* and lead to misclassifications. Finally, we were able to improve the accuracy of the classification by removing or masking out ecologically irrelevant classes such as built-up areas, roads, and agricultural fields. This is because the bright signals of these classes often interfered with vegetation classes, especially when the glare from water caused misclassifications and reduced the overall accuracy.

We were relatively successful in classifying *Phragmites* stands according to height and weight. When *Phragmites* stands are dense, they produced purer reflectance signals that were not mixed with those of other classes. Mature *Phragmites* can grow up to 3–4 m high and reach densities of 200 live and 300 dry stands per square meter under optimal conditions (Hara et al. 1993; Poulin et al. 2010). Optimal conditions for *Phragmites* are freshwater bodies with seasonal fluctuations of 30 cm (Deegan et al. 2007) and all our study sites provide these ideal conditions

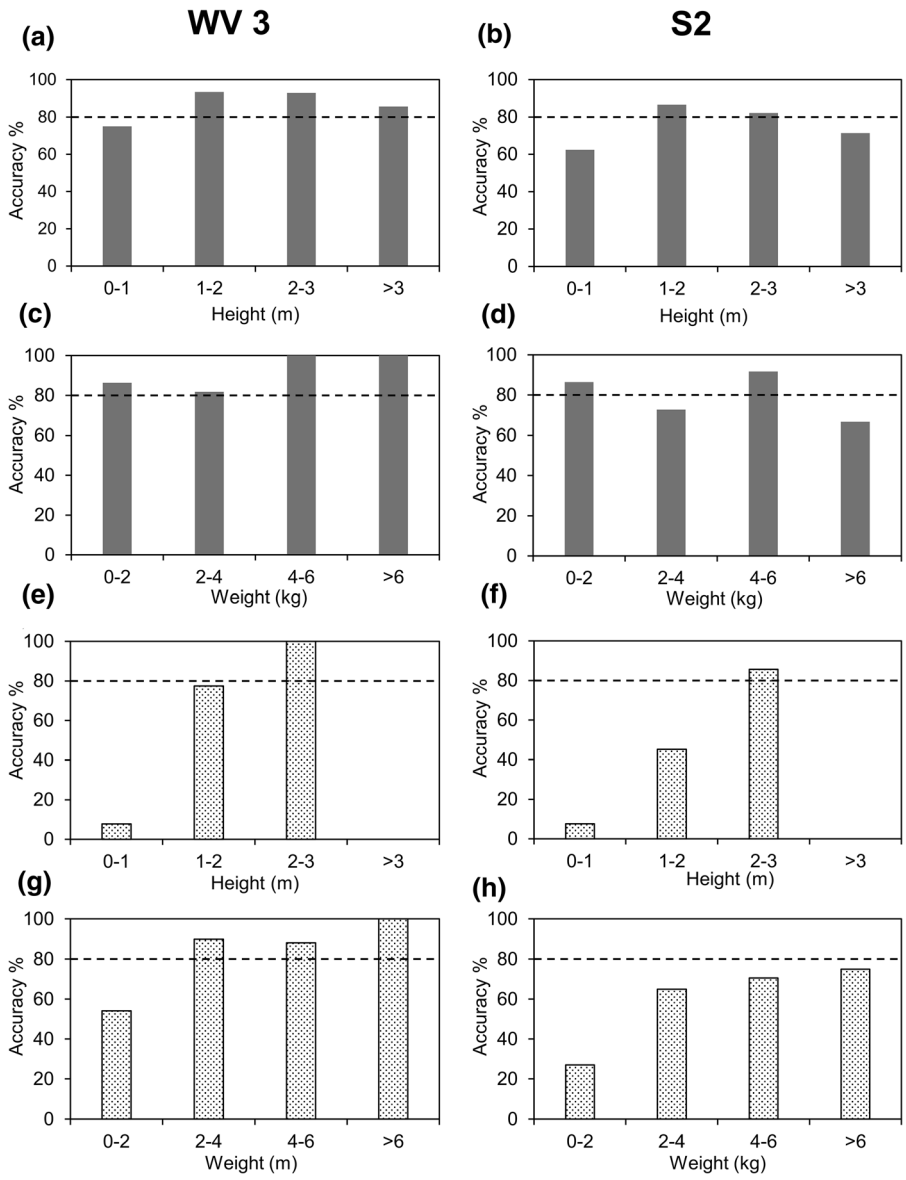

Fig. 8 Mapping accuracies of height and weight of *Phragmites* for BCNWA (solid bars) and CM (stippled bars) using WV3 (all left panels) and S2 (all right panels). (Note: no data for > 3 m height category in CM site)

for *Phragmites* colonization. According to Hara et al. (1993), *Phragmites* does not increase shoot diameter, and increase in shoot weight is parallel to increase in shoot height. At younger stages, *Phragmites* shoots use carbohydrates from the rhizomes, accumulated during the previous growing season. Therefore, younger shoots are smaller and have fewer number of small leaves (Hara et al. 1993). Furthermore, density and height of *Phragmites* stands could also be affected by environmental conditions such as water level fluctuations. We obtained acceptable accuracy for even the lowest height and weight category with the WV3 images. Our study confirms that WV2/3 could be effectively used for mapping even young or smaller *Phragmites* stands; however, S2 could only be used to map older, denser, or larger *Phragmites* stands with less spectral mixing.

Timing of image acquisition and plant phenology are important considerations in *Phragmites* mapping (Rupasinghe and Chow-Fraser 2019). *Phragmites*

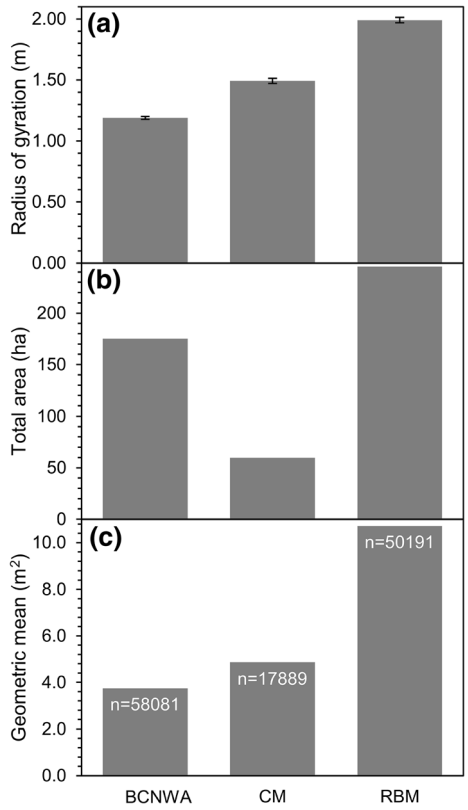

Fig. 9 Comparison of **a** mean Radius of Gyration, **b** mean total area occupied by *Phragmites* and **c** geometric mean size of *Phragmites* stands in the three wetlands in this study. Data were calculated from classification of WV2/3 images with the ML classification

produce the most unique, detectable signal that can be separated from other vegetation classes (especially Cattail and meadow marsh) during the peak summer period. The distinct inflorescence, the unique green color due to the high chlorophyll concentration, the leaf arrangement, and the high water-use efficiency of *Phragmites* during this period all could be combined to produce this unique spectral signature. Use of images collected in late summer is also beneficial as the *Phragmites* treatment is usually conducted in September to October and this provides most up-to-date map. Use of Short-Wave IR bands may also improve the classification accuracy (Rupasinghe and Chow-Fraser 2019). One obvious limitation of WV2/3 is the potentially high cost of acquiring images to map large invasion areas.

We have shown that besides differences in resolution of satellite images, we can attribute some of the variation in mapping accuracies among the three sites to differences in treatment history along with amount of field data, and the timing of image acquisition. Since the entire CM had been treated in the fall of 2017 and the image was acquired in July the following year, there were no mature stands but many small stands that had either escaped treatment or had recently regenerated. Therefore, there was interference from water reflectance in many inundated areas that were absent in the other two sites. By comparison, mature stands in the diked area of BCNWA could be mapped accurately because they were large and dense and had not yet been treated at the time of image acquisition. We had relatively few RBM data to train and validate the classification of small sparse stands of common reed, whereas such data had been specifically collected in CM and BCWNA, and this may also explain differences in mapping accuracies. According to Rupasinghe and Chow-Fraser (2019), images acquired in July and early August was best for minimizing confusion between *Phragmites* and *Typha* and were associated with highest accuracies for *Phragmites*. Therefore, all else being equal, the July image for LP could explain the better performance than the September image for RBM.

Conclusion

Tracking *Phragmites* distribution, determining the borders of the patches, and estimating the extent of invaded area are common objectives of invasive plant management programs. The conventional approach is to map the distribution using field surveys, which are extremely labour intensive, and which may produce results that are biased against smaller and mixed *Phragmites* stands depending on the thoroughness of the observer. Mapping approaches with remote sensing technology can overcome these challenges by providing comprehensive coverage of both small and large study areas, even if they are difficult to access by boat or by road. Accurate distribution of relatively small *Phragmites* stands are difficult to obtain, but they are very valuable to managers because both mechanical and chemical treatment are most effective when populations are small and sparsely distributed. Using commercially purchased high-resolution satellite images, we were able to map younger, less dense, or smaller *Phragmites* stands as well as the mature,

dense, and larger *Phragmites* stands with overall accuracy greater than 80%. By comparison, satellite images from S2 that are available at no cost could be used to accurately map large, high density *Phragmites* stands, but this approach is only useful when general estimation of *Phragmites* cover is required over large spatial extents. The mapping accuracy is dependent on the *Phragmites* patch characteristics, other wetland plant species, and the site conditions. We recommend masking out ecologically irrelevant or adjacent land-cover classes (e.g. agricultural lands, roads, and buildings) to reduce classification errors and computational time. Use of spectral unmixing of WV2/3 is a promising method for detection of *Phragmites* in wetlands, especially for detecting new *Phragmites* growth in treated areas and for routine mapping and regular updating purposes.

Acknowledgements Authors would like to thank Dr. James Marcaccio, Jordan DeBoer, and Dr. Chantel Markle for support with UAV image acquisition and field data collection. We would like to thank Jennifer Angoh (Trent University) and Dr. Christina Davy (Trent University and Ontario Ministry of Natural Resources and Forestry) for sharing field data from the RBM site. We are grateful to the Nature Conservancy of Canada for providing partial funding for this study. We would also like to thank Canadian Wildlife Service and Ministry of Environment and Climate Change Canada for providing permission to conduct field work at the BCNWA site. We are grateful to the Nature Conservancy of Canada and Parks Ontario for the *Phragmites* treatment locations data for this study. We would like to express our gratitude to the reviewers and Associate Editor for providing valuable comments and suggestions to improve our manuscript.

Author contributions All authors contributed to the study conception and design. Data collection and image processing were conducted by Prabha A. Rupasinghe and the data analysis was performed by both authors, Prabha A. Rupasinghe and P. Chow-Fraser. The first draft of the manuscript was written by Prabha A. Rupasinghe and P. Chow-Fraser commented and contributed to previous versions of the manuscript. All authors read and approved the final manuscript.

Funding This study was partially funded by the Nature Conservancy of Canada (NCC).

Availability of data and materials WV2/3 images analysed during the current study are not publicly available because they are only licensed for use by researchers at McMaster University; ground reference data were collected and/or shared by a number of other agencies and institutions specifically for this study only (Please refer to the acknowledgment section for further details). Individuals interested in interim or final data and details of procedures should contact the corresponding author with a written request.

Code availability No custom codes are developed during the study. All image processing and analysis were conducted using pre-built tools in number of software; ENVI 5.5, ArcMap 10.4.1, Fragstats 4.2, JMP 15, and MS Excel. Please refer to the methods section for further details.

Compliance with ethical standards

Conflict of interest The authors declare that they have no conflict of interest.

References

Adam E, Mutanga O, Rugege D (2010) Multispectral and hyperspectral remote sensing for identification and mapping of wetland vegetation: a review. Wetl Ecol Manag 18:281–296. https://doi.org/10.1007/s11273-009-9169-z

Adams JB, Smith MO, Johnson PE (1985) Spectral mixture modeling: a new analysis of rock and soil types at the Viking Lander 1 site. J Geophys Res 91:8098–8112. https://doi.org/10.1029/JB091iB08p08098

Ailstock MS, Norman CM, Bushmann PJ (2001) Common reed *Phragmites australis*: control and effects upon biodiversity in freshwater nontidal wetlands. Restor Ecol 9:49–59. https://doi.org/10.1046/j.1526-100x.2001.009001049.x

Albert A, Brisson J, Belzile F et al (2015) Strategies for a successful plant invasion: the reproduction of *Phragmites australis* in north-eastern North America. J Ecol 103:1529–1537. https://doi.org/10.1111/1365-2745.12473

Avers B, Fahlsing R, Kafcas E, et al (2007) A guide to the control and management of invasive *Phragmites*. Mich Dep Environ Qual Lansing

Bachmann CM, Donato TF, Lamela GM et al (2002) Automatic classification of land cover on Smith Island, VA, using HyMAP imagery. IEEE Trans Geosci Remote Sens 40:2313–2330. https://doi.org/10.1109/TGRS.2002.804834

Boardman JW (1998) Leveraging the high dimensionality of AVIRIS data for improved sub-pixel target unmixing and rejection of false positives: mixture tuned matched filtering. In: Summaries of the seventh JPL Airborne Geoscience Workshop, JPL Publication, 1998. NASA Jet Propulsion Laboratory, pp 55–56

Boardman JW, Kruse FA (2011) Analysis of imaging spectrometer data using N-dimensional geometry and a mixture-tuned matched filtering approach. IEEE Trans Geosci Remote Sens 49:4138–4152. https://doi.org/10.1109/TGRS.2011.2161585

Boardman JW, Kruse FA, Green RO (1995) Mapping target signatures via partial unmixing of AVIRIS data. In: JPL airborne Earth science workshop, pp 23–26

Bolton RM, Brooks RJ (2010) Impact of the seasonal invasion of *Phragmites australis* (common reed) on turtle reproductive success. Chelonian Conserv Biol 9:238–243. https://doi.org/10.2744/CCB-0793.1

Bourgeau-Chavez L, Endres S, Battaglia M et al (2015) Development of a bi-national Great Lakes coastal wetland and land use map using three-season PALSAR and Landsat

imagery. Remote Sens 7:8655–8682. https://doi.org/10.3390/rs70708655

Brelsford C, Shepherd D (2013) Using mixture tuned match filtering to measure changes in subpixel vegetation area in Las Vegas, Nevada. In: Remote sensing and modeling of ecosystems for sustainability X. International Society for Optics and Photonics, San Diego, California, United States, p 88690B

Brisson J, de Blois S, Lavoie C (2010) Roadside as invasion pathway for common reed (*Phragmites australis*). Invasive Plant Sci Manag 3:506–514. https://doi.org/10.1614/IPSM-09-050.1

Burgess ND, Evans CE (1989) The management of reedbeds for birds. Information Press, Oxford

Campbell JB (2002) Introduction to remote sensing, 3rd edn. The Guilford Press, New York

Chambers RM, Meyerson LA, Saltonstall K (1999) Expansion of *Phragmites australis* into tidal wetlands of North America. Aquat Bot 64:261–273. https://doi.org/10.1016/S0304-3770(99)00055-8

Cook CE, McCluskey AM, Chambers RM (2018) Impacts of invasive *Phragmites australis* on diamondback terrapin nesting in Chesapeake Bay. Estuaries Coasts 41:966–973. https://doi.org/10.1007/s12237-017-0325-z

Deegan BM, White SD, Ganf GG (2007) The influence of water level fluctuations on the growth of four emergent macrophyte species. Aquat Bot 86:309–315. https://doi.org/10.1016/j.aquabot.2006.11.006

Derr JF (2008) Common reed (*Phragmites australis*) response to mowing and herbicide application. Invasive Plant Sci Manag 1:12–16. https://doi.org/10.1614/IPSM-07-001.1

European Space Agency (2020) Sentinel-2 missions resolution and swath sentinel handbook. https://sentinel.esa.int/web/sentinel/missions/sentinel-2/instrument-payload/resolution-and-swath. Accessed 2 Mar 2020

Finkelstein SA, Davis AM (2006) Paleoenvironmental records of water level and climatic changes from the middle to late holocene at a Lake Erie coastal wetland, Ontario, Canada. Quat Res 65:33–43. https://doi.org/10.1016/j.yqres.2005.08.021

Gagnon Lupien N, Gauthier G, Lavoie C (2015) Effect of the invasive common reed on the abundance, richness and diversity of birds in freshwater marshes. Anim Conserv 18:32–43. https://doi.org/10.1111/acv.12135

Garmin, subsidiaries GL or its Garmin eTrex® 10 | Outdoor GPS. In: Garmin. https://buy.garmin.com/en-CA/CA/p/87768. Accessed 18 Apr 2020

Gilbert J (2015) Rondeau provincial park invasive *Phragmites* management program 2008–2014 summary report and recommended next steps

Gilbert J, Vidler N, Cloud Sr P, et al (2014) *Phragmites australis* at the crossroads: why we cannot afford to ignore this invasion. In: Proceedings of great lakes wetlands day. Toronto, ON, Canada, pp 78–84

Hara T, van Der Toorn J, Mook JH (1993) Growth dynamics and size structure of shoots of *Phragmites Australis*, a Clonal Plant. J Ecol 81:47–60. https://doi.org/10.2307/2261223

Harris Geospatial Solutions, Inc (2020) Mixture tuned matched filtering. https://www.harrisgeospatial.com/docs/MTMF.html. Accessed 21 Mar 2020

Kurihara J, Takahashi Y, Sakamoto Y et al (2018) HPT: a high spatial resolution multispectral sensor for microsatellite remote sensing. Sensors. https://doi.org/10.3390/s18020619

L3Harris Geospatial (2020) ENVI—The leading geospatial image analysis software. https://www.harrisgeospatial.com/Software-Technology/ENVI. Accessed 25 Mar 2020

Lambert AM, Dudley TL, Saltonstall K (2010) Ecology and impacts of the large-statured invasive grasses *Arundo donax* and *Phragmites australis* in North America. Invasive Plant Sci Manag 3:489–494. https://doi.org/10.1614/IPSM-D-10-00031.1

Lass LW, Prather TS, Glenn NF et al (2005) A review of remote sensing of invasive weeds and example of the early detection of spotted knapweed (*Centaurea maculosa*) and baby's breath (*Gypsophila paniculata*) with a hyperspectral sensor. Weed Sci 53:242–251. https://doi.org/10.1614/WS-04-044R2

Lathrop RG, Windham L, Montesano P (2003) Does *Phragmites* expansion alter the structure and function of marsh landscapes? Patterns and processes revisited. Estuaries 26:423–435. https://doi.org/10.1007/BF02823719

Long Point Crown Marsh Rehabilitation Steering CommitteeLong Point Crown Marsh Rehabilitation Steering Committee (2007) Toward Rehabilitation of the Crown Marsh - Long Point, Lake Erie, Ontario. Ontario Ministry of Natural Resources, University of Western Ontario, Long Point Waterfowl and Wetlands Research Fund, Long Point Waterfowlers Association, Bird Studies Canada, Bird Studies Canada

Lopez RD, Edmonds CM, Neale AC, et al (2004) Accuracy assessments of airborne hyperspectral data for mapping opportunistic plant species in freshwater coastal wetlands. In: Lunetta RS, Lyon JG (eds)In remote sensing and GIS accuracy assessment. CRC Press, Boca Raton, pp 253–267

Mal TK, Narine L (2004) The biology of Canadian weeds. 129. *Phragmites australis* (Cav.) Trin. ex Steud. Can J Plant Sci 84:365–396. https://doi.org/10.4141/P01-172

Mann DL, Nelson JG (1980) Ideology and wildlands management: the case of Rondeau Provincial Park, Ontario. Environ Manage 4:111–124. https://doi.org/10.1007/BF01866508

Marcaccio JV, Markle CE, Chow-Fraser P (2016) Use of fixed-wing and multi-rotor unmanned aerial vehicles to map dynamic changes in a freshwater marsh. J Unmanned Veh Syst 4:193–202. https://doi.org/10.1139/juvs-2015-0016

Markle CE, Chow-Fraser P (2018) Effects of European common reed on Blanding's turtle spatial ecology. J Wildl Manag 82:857–864. https://doi.org/10.1002/jwmg.21435

Marks M, Lapin B, Randall J (1994) *Phragmites australis* (*P. communis*): threats, management and monitoring. Nat Areas J 14:285–294

McNabb CD, Batterson TR (1991) Occurrence of the common reed, *Phragmites australis*, along roadsides in Lower Michigan. Mich Acad USA 23:211–220

Meyerson LA, Saltonstall K, Windham L et al (2000) A comparison of *Phragmites australis* in freshwater and brackish marsh environments in North America. Wetl Ecol Manag 8:89–103. https://doi.org/10.1023/A:1008432200133

Ministry of Natural Resources and Forestry (2019) Invasive Phragmites Control at Long Point Region and Rondeau

Provincial Park Implementation Plan—2019 Ministry of Natural Resources and Forestry Ministry of Environment, Conservation and Park, Canadian Wildlife Service

Nikolakopoulos K, Oikonomidis D (2015) Quality assessment of ten fusion techniques applied on Worldview-2. Eur J Remote Sens 48:141–167. https://doi.org/10.5721/EuJRS20154809

Phillips RL, Beeri O, DeKeyser ES (2005) Remote wetland assessment for Missouri Coteau prairie glacial basins. Wetlands 25:335–349

Poulin B, Davranche A, Lefebvre G (2010) Ecological assessment of *Phragmites australis* wetlands using multi-season SPOT-5 scenes. Remote Sens Environ 114:1602–1609. https://doi.org/10.1016/j.rse.2010.02.014

Rodríguez M, Brisson J (2015) Pollutant removal efficiency of native versus exotic common reed (*Phragmites australis*) in North American treatment wetlands. Ecol Eng 74:364–370. https://doi.org/10.1016/j.ecoleng.2014.11.005

Rupasinghe PA, Chow-Fraser P (2019) Identification of most spectrally distinguishable phenological stage of invasive *Phramites australis* in Lake Erie wetlands (Canada) for accurate mapping using multispectral satellite imagery. Wetl Ecol Manag 27:513–538. https://doi.org/10.1007/s11273-019-09675-2

Rupasinghe P, Markle C, Marcaccio J, Chow-Fraser P (2017) Determination of treatment effectiveness of *Phragmites autralis* at Rondeau Bay Provincial Park, ON. In: Proceedings of CASIOPA. Georgian Bay Hotel and Conference Centre, Collingwood, ON, p 24

Rutchey K, Vilchek L (1999) Air photointerpretation and satellite imagery analysis techniques for mapping cattail coverage in a northern Everglades impoundment. Photogramm Eng Remote Sens 65:185–191

Saltonstall K (2002) Cryptic invasion by a non-native genotype of the common reed, P*hragmites australis*, into North America. Proc Natl Acad Sci 99:2445–2449. https://doi.org/10.1073/pnas.032477999

Satellite Image Corporation (2017a) WorldView-3 Satellite Sensor. https://www.satimagingcorp.com/satellite-sensors/worldview-3/. Accessed 2 Mar 2020

Sawaya KE, Olmanson LG, Heinert NJ et al (2003) Extending satellite remote sensing to local scales: land and water resource monitoring using high-resolution imagery. Remote Sens Environ 88:144–156. https://doi.org/10.1016/j.rse.2003.04.006

Schmidt KS, Skidmore AK (2001) Exploring spectral discrimination of grass species in African rangelands. Int J Remote Sens 22:3421–3434. https://doi.org/10.1080/01431160152609245

SenseFly (2020a) senseFly—eBee Classic. In: senseFly. https://www.sensefly.com/homepage/ebee-small. Accessed 18 Apr 2020

SenseFly (2020b) senseFly—Parrot Sequoia+. In: senseFly. https://www.sensefly.com/camera/parrot-sequoia. Accessed 18 Apr 2020

Taddeo S, Blois SD (2012) Coexistence of introduced and native common reed (*Phragmites australis*) in freshwater wetlands. Écoscience 19:99–105. https://doi.org/10.2980/19-2-3468

Uddin MN, Robinson RW, Caridi D, Al Harun MAY (2014) Suppression of native *Melaleuca ericifolia* by the invasive *Phragmites australis* through allelopathic root exudates. Am J Bot 101:479–487. https://doi.org/10.3732/ajb.1400021

Vretare V, Weisner SE, Strand JA, Granéli W (2001) Phenotypic plasticity in *Phragmites australis* as a functional response to water depth. Aquat Bot 69:127–145. https://doi.org/10.1016/S0304-3770(01)00134-6

Weinstein MP, Balletto JH (1999) Does the common reed, *Phragmites australis*, affect essential fish habitat? Estuaries 22:793–802. https://doi.org/10.2307/1353112

Weisner SEB, Strand JA (1996) Rhizome architecture in *Phragmites australis* in relation to water depth: implications for within-plant oxygen transport distances. Folia Geobot 31:91–97. https://doi.org/10.1007/BF02803998

Wilcox KL, Petrie SA, Maynard LA, Meyer SW (2003) Historical distribution and abundance of *Phragmites australis* at long point, Lake Erie, Ontario. J Gt Lakes Res 29:664–680. https://doi.org/10.1016/S0380-1330(03)70469-9

Williams AP, Hunt ER Jr (2002) Estimation of leafy spurge cover from hyperspectral imagery using mixture tuned matched filtering. Remote Sens Environ 82:446–456. https://doi.org/10.1016/S0034-4257(02)00061-5

Williams AEP, Hunt ER Jr (2004) Accuracy assessment for detection of leafy spurge with hyperspectral imagery. Rangel Ecol Manag 57:106–112. https://doi.org/10.2111/1551-5028(2004)057[0106:AAFDOL]2.0.CO;2

Yuckin S, Rooney R (2019) Significant increase in nutrient stocks following *Phragmites australis* invasion of freshwater meadow marsh but not of Cattail Marsh. Front Environ Sci. https://doi.org/10.3389/fenvs.2019.00112